Heliyon 9 (2023) e19855

Contents lists available at ScienceDirect

Heliyon

journal homepage: www.cell.com/heliyon

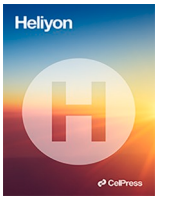

Restriction-ligation-independent production of a TVCV infectious clone and a TVCV-based gene expression vector

Andrea Mirauti, Phu-Tri Tran, Vitaly Citovsky *

Department of Biochemistry and Cell Biology, State University of New York, Stony Brook, NY 11794-5215, USA

ARTICLE INFO

Keywords:
TVCV infectious clone
Restriction-ligation-independent cloning
TVCV gene expression vector

ABSTRACT

Transgenic expression of proteins in plants is central to research and biotechnology, and, often, it is desirable to obtain this expression without altering the nuclear or plastid genomes. Thus, expression vectors based on plant viruses that infect multiple cells are useful; furthermore, they are also advantageous for studies of the life cycle of the virus itself. Here, we report the development of an expression vector based on a *Turnip vein-clearing virus* (TVCV), a tobamovirus known to easily infect two model plants, *Nicotiana benthamiana*, and *Arabidopsis thaliana*. Avoiding restriction digestion, we utilized a restriction-ligation-independent cloning approach to construct an infectious cDNA clone of TVCV from the viral RNA and then to convert this clone to a gene expression vector adapted for Gateway-based recombination cloning for transgene insertion. The functionality of the resulting vector, designated pTVCV-DEST, was validated by the expression of an autofluorescent reporter transgene following agroinoculation of the target plant.

1. Introduction

Production of proteins of interest in plants has evolved as one of the major tools for plant biology research and biotechnology applications, from agriculture to biopharming. Furthermore, in many cases, it would be useful to achieve this transgenic expression without altering the nuclear or plastid genomes of the plant, avoiding public concerns over genetically modified organisms. To achieve this goal, a relatively long line of plant gene expression vectors has been developed based on plant viruses that infect multiple cells and express high amounts of proteins yet do not integrate into the host cell genetic material [1–4]. Obviously, such plant virus expression vectors can be used not only for protein-based applications but also for virus-induced gene silencing (VIGS) [4].

Already almost four decades ago, a plant DNA pararetrovirus, Cauliflower mosaic virus (CaMV), was used as a vector to express a heterologous gene in plants [5]. Since then, several diverse groups of plant viruses have been recruited to the list of virus-based vectors for gene expression in plants. Among these, geminiviruses are used most often for DNA virus-based vectors whereas RNA virus-based vectors are more diverse and include tobraviruses, potyviruses, potexviruses, comoviruses, and tobamoviruses [2,3]. Virus-based expression vectors are also useful for studies of the life cycle of the same viruses themselves, allowing, for example, direct tagging of the infected cells. Many such studies involve tobamoviruses as a model virus and *Nicotiana benthamiana* or *Arabidopsis thaliana* as model plants, and they would benefit from an expression vector based on a tobamovirus that easily infects both *N. benthamiana* and Arabidopsis. The paradigm for such tobamoviruses is the *Turnip vein-clearing virus* (TVCV) [6–9]. TVCV is a positive-strand RNA virus that belongs to subgroup 3 of tobamoviruses [10–12]; noteworthy, the members of this subgroup display greater overlap between their

* Corresponding author.
E-mail address: vitaly.citovsky@stonybrook.edu (V. Citovsky).

https://doi.org/10.1016/j.heliyon.2023.e19855
Received 2 February 2023; Received in revised form 20 August 2023; Accepted 4 September 2023
Available online 5 September 2023

movement (MP) and coat protein (CP) genes compared to subgroups 1 and 2 [11], resulting in further compression and strengthening of subgenomic promoters and, potentially, benefitting vector stability and transgene expression.

Here, we took advantage of the concept of restriction-ligation-independent cloning [13–17] to produce an infectious clone of TVCV, pTVCV, and its variation expressing a GFP tag, pTVCV-GFP. Unlike standard cloning approaches which increase the complexity and labor intensity of cloning projects, restriction-ligation-independent cloning allows one-step cloning of 2–4 long DNA fragments by annealing their single-stranded overhangs produced the 3′→5′ exonuclease "chew-back" activity of T4 DNA polymerase in the absence of one of the four nucleotides [18]. The annealed fragments are ligated in *E. coli* by the endogenous bacterial DNA repair machinery [14,15]. pTVCV generated by this approach was then adapted for Gateway-based recombination cloning, allowing its use as a plant gene expression vector, designated pTVCV-DEST. In this construct, a heterologous TMV CP promoter drives the expression of the gene of interest, placed upstream of the TVCV MP sequence without disturbing the overlapping area of the CP and MP genes to preserve the native viral infectivity. All three constructs were infectious in *N. benthamiana* and *Arabidopsis* plants. For further functional validation, an ER-targeted mRFP reporter was cloned into pTVCV-DEST and expressed in plant tissues. In addition to the production of the pTVCV-DEST vector, restriction-ligation-independent cloning may serve as a new approach for the assembly of infectious clones of plant RNA viruses newly isolated from nature.

2. Materials and methods

2.1. Plant material

Nicotiana benthamiana and *Arabidopsis thaliana* (ecotype Col-0) plants were maintained in a growth chamber at 23 °C with a relative humidity of 50–60% under a 16:8-h ratio of light to dark photoperiod with a light intensity of 100 μmol photons m^{-2} s^{-1}. These conditions are based on the plant growth protocols routinely employed in our laboratory [19–21]. After two weeks of growth, the plants were utilized for agroinoculation of the tested vectors.

2.2. Vector construction by restriction-ligation-independent cloning

To generate the template for amplification of the TVCV genomic RNA, the total RNA from *N. benthamiana* leaf tissues infected with pTVCV50, which contains the full-length infectious TVCV cDNA clone [22], was extracted with the TRIzol reagent (Invitrogen) according to the manufacturer's instructions. The purified total RNA served as a template for the synthesis of the TVCV cDNA using the RevertAid Reverse Transcription Kit (Thermofisher) and random hexamer primers. Then, overlap-extension PCR (overlap PCR) was performed using PfuUltra II Fusion HS DNA polymerase (Agilent) in the C1000 thermal cycler (Bio-Rad). The nucleotide sequences of all primers used in this study are listed in Table S1. In detail, four PCR fragments for the construction of the vector were generated as follows: 2260-bp PCR1 was amplified from pJL-TRBO (plasmid #80082, Addgene) [23] with primers 1 and 2; 2608-bp PCR2 was amplified by overlap PCR with primers 3 and 6 using pJL-TRBO (1017 bp fragment, amplified with primers 3 and 4), and TVCV cDNA (1615-bp fragment, amplified with primers 5 and 6); 2747-bp PCR3 was amplified from TVCV cDNA with primers 7 and 8; The PCR4 fragment, containing the expression cassette, varied between the pTVCV, pTVCV-GFP, and pTVCV-DEST constructs. For pTVCV, 3430-bp PCR4 was amplified by overlap PCR with primers 9 and 12 from TVCV cDNA (2037-bp fragment, amplified with primers 9 and 10) and pJL-TRBO (1417-bp fragment, amplified with primers 11 and 12). For pTVCV-GFP, 4741-bp PCR4 was amplified by overlap PCR with primers 9 and 12 from three fragments: a 613-bp fragment (amplified from TVCV cDNA with primers 9 and 13), a 1151-bp fragment (amplified from pJL-TRBO-G (plasmid #80083, Addgene) [23] with primers 14 and 15), and a 3026-bp fragment (amplified from pTVCV with primers 12 and 16). For pTVCV-DEST, 5813-bp PCR4 also was amplified by overlap PCR with primers 9 and 12 from three fragments: a 798-bp fragment (amplified from pTVCV-GFP with primers 9 and 17), a 2223-bp fragment (amplified from pSK104 [24] with primers 14 and 15), and the 3026-bp fragment (amplified from pTVCV-GFP with primers 12 and 16). The thermal cycler program comprised initial denaturation at 95 °C for 2 min followed by 30 cycles at 95 °C for 20 s, 58 °C for either 30 s (for PCR1 and PCR3) or 5 min (for PCR2 and PCR4), and 72 °C for either 30 s (for PCR1 and PCR3) or 1 min (for PCR2 and PCR4), and the final extension at 72 °C for 5 min.

The PCR1-4 fragments were then combined in a variation of the restriction-ligation-independent cloning protocol [13] to construct binary plasmids that contain the TVCV-based sequences between the left and right T-DNA borders. To this end, the fragment pairs PCR1/PCR3 and PCR2/PCR4 were treated at 27 °C for 5 min with T4 DNA polymerase in the presence of dTTP or dATP, respectively; the reaction was then cooled down at 4 °C for 5 min, and the enzyme was inactivated by incubation at 75 °C for 20 min. The treated fragment pairs (5 μl) were mixed with each other and incubated at 55 °C for 30 min and then at 25 °C overnight to allow annealing, followed by the introduction of the annealed vector (50–100 ng) into the *E. coli* strain PB3.1 (NCBI accession NZ_JACFYE000000000.1) and propagated on LB agar supplemented with 100 μg/ml kanamycin and 25 μg/ml chloramphenicol. All constructs were confirmed by DNA sequencing.

2.3. Gateway recombination cloning of the ER-targeted mRFP reporter transgene into pTVCV-DEST

The entry clone pDONR207-ER-mRFP was made by the BP reaction cloning of the AttB PCR product of the ER-mRFP coding sequence into pDONR207 (Invitrogen); the ER-mRFP template was derived from pImpactVector1.3-ER-mRFP, which is pImpact-Vector1.3 (Plant Research International, Wageningen, The Netherlands) encoding the ER signal peptide (SLSQNQAKFSKGFVV-MIWVLFIACAITSTEAS) fused to the amino terminus of mRFP derived from the p2999 plasmid (kindly provided by Dr. Stanton Gelvin,

Purdue University).

Then, ER-mRFP coding sequence was transferred from pDONR207-ER-mRFP to pTVCV-DEST by the LR reaction as described by the manufacturer, with slight modifications. Specifically, in a 20-μl reaction, 150 ng of pDONR207-ER-mRFP was mixed with 300 ng of pTVCV-DEST and 2 μl of LR clonase (Invitrogen), incubated at 25 °C overnight and treated for 10 min at 37 °C with 1 μl of proteinase K (>600 U/ml, Invitrogen) to inactivate the enzyme. The resulting construct pTVCV-DEST-ER-mRFP was confirmed by DNA sequencing. Gateway-based plasmids were maintained in the DB3.1 strain of *E. coli* (Invitrogen); this strain harbors the *gyrA462* gene which generates resistance to the toxicity of the *ccdB* gene [25].

2.4. Agrobacterium-mediated inoculation

Each tested binary vector, i.e., pTVCV, pTVCV-GFP, pTVCV-DEST, and pTVCV-DEST-Er-mRFP, was transformed into *Agrobacterium tumefaciens* strain EHA105 [26,27]. Agroinoculation of *N. benthamiana* and Arabidopsis leaves was performed as described [28,29], respectively. Briefly, Agrobacterium cells harboring the tested construct were grown in liquid LB medium at 28 °C overnight, collected by centrifugation at 000×*g* at 25 °C for 10 min, and resuspended to an $OD_{600} = 0.2$ in MMA (10 mM $MgCl_2$, 10 mM MES pH 5.6, 100 μM acetosyringone). Two fully expanded leaves were agroinoculated using 1-ml needleless syringes. The plants were then placed into growth chambers and observed for signs of infection and recorded with a digital camera. Each inoculation was repeated three times.

GFP expression in the whole plants agroinoculated with pTVCV-GFP was visualized 6 days post inoculation (dpi) in the upper, uninoculated leaves by irradiation with the long-wave UV light (366 nm) using the Model UVGL-25 Mineralight® lamp, and the GFP fluorescence was recorded using a digital camera equipped with a UV filter (Sony). GFP and ER-mRFP expression within cells of the plants agroinfected with pTVCV-GFP or pTVCV-DEST-ER-mRFP was visualized using a confocal laser scanning microscope (LSM 900, Zeiss, Germany) with GFP and RFP filters. Specifically, for GFP detection, we used a solid-state laser excitation line at 488 nm and an emission filter at 410–617 nm; for RFP detection, we used a solid-state laser excitation line at 590 nm and an emission filter at 410–617 nm; and for detection of the plastid autofluorescence, we used a solid-state laser excitation line at 488 nm and an emission filter at 624–700 nm.

2.5. Reverse transcription-quantitative PCR (RT-qPCR)

Total RNA was extracted from upper, uninoculated leaves of *N. benthamiana* using TRIzol and utilized as a template for the synthesis of cDNA using the RevertAid Revert Transcription Kit and Hexa-random primers. For quantification of pTVCV RNA, 50 mg of leaf tissue was harvested at 6 dpi and, for quantification of GFP expression, 100 mg of leaf tissue was harvested at 14 dpi. qPCR was performed using the EvaGreen Dye protocol (Gold Biotechnology) per the manufacturer's instructions in a MiniOpticon real-time PCR system (Bio-Rad). The healthy, uninfected plants were used as a negative control, and the pTVCV-inoculated plants were used as a positive control. Fold enrichment for each reaction was calculated by the delta-delta Ct (cycle threshold, i.e., the number of amplification cycles when the specific signal becomes detectable) method as described [30,31], and presented relative to that in the mock-inoculated plants, which was set to 1.0. The *Actin* gene of *A. thaliana* was used as a reference gene. Specific primers used in these experiments are detailed in Table S1.

2.6. Western blotting

The pTVCV-DEST vector is designed to fuse a 3xFLAG epitope to the amino terminus of the expressed protein; therefore, we analyzed the accumulation of the ER-mRFP protein in the expressing tissues by Western blotting using anti-FLAG antibodies. To this end, total proteins were extracted from the *N. benthamiana* leaves agroinoculated with pTVCV-DEST-ER-mRFP at 14 dpi using TRIzol and resolved by SDS polyacrylamide gel electrophoresis (PAGE) on a 12% gel and electro-blotted onto a PVDF membrane (Immobilon). The large unit of RuBisCo was used as the loading control and detected on the blots by the Ponceau S (Sigma-Aldrich) staining. The blots were blocked with casein (1%, pH 8 in the TBS-T buffer), probed with monoclonal anti-FLAG M2 antibody (Sigma-Aldrich, F1804-50UG), followed by the horseradish peroxidase-conjugated goat anti-mouse IgG antibody (Promega, W4028), analyzed using an Opti-4CN Substrate Kit (Bio-Rad), and recorded using a Gel Doc XR+ gel documentation system (Bio-Rad).

2.7. Quantification and statistical analysis

All representative images reflect a minimum of three biological replicates. All quantitative data were derived from 3 biological replicates and 2 technical repeats. The statistical significance of differences in sample means was evaluated by the two-tailed unpaired *t*-test using Excel 365 (Microsoft) software, with *P*-values < 0.05 or 0.01, corresponding to the statistical probability of >95% or 99%, respectively, considered statistically significant.

3. Results and discussion

3.1. Construction of an infectious TVCV clone by restriction-ligation-independent cloning

We decided to begin our construction of a TVCV-based expression vector from *de novo* production of an infectious TVCV cDNA clone directly from the viral genomic RNA isolated from the infected plant tissues using a restriction-ligation-independent strategy

[13–17]. So far, this technique has not been deployed for the generation of plant virus infectious clones, yet its technical and conceptual advantages would clearly benefit the assembly of infectious clones of any newly isolated plant RNA viruses. Specifically, traditional restriction- and ligation-based cloning methods are often low-efficiency and time-consuming [16] and are complicated by incomplete restriction digestion, effects of DNA methylation, and, at times, a limited selection of the appropriate restriction endonuclease recognition sites within viral sequences. Obviously, restriction-ligation-independent cloning circumvents these potential difficulties; instead, it relies on the natural DNA repair systems of *E. coli* cells [14,15].

Fig. 1A shows that the application of this restriction-ligation-independent cloning technique to the TVCV cDNA produced four PCR fragments which represented the building blocks of the complete binary vector carrying the infectious TVCV clone. These PCR fragments were treated with T4 DNA polymerase, which, due to its 3′→5′ exonuclease activity, generates >20 nucleotide-long recessed DNA ends that are longer than those achieved by many restriction endonucleases and, thus, are more conducive to fragment annealing. After the PCR1-4 fragments were annealed, they were introduced into *E. coli* cells (Fig. 1A), which repaired the breaks between the fragments, producing a complete vector construct. Importantly, in our hands, this technique had 100% efficiency as all *E. coli* colonies grown after the transformation and antibiotic selection contained the complete and correct constructs. Using this approach, we produced two variations of the TVCV infectious clone, pTVCV and pTVCV-GFP, both incorporated in a pJL-TRBO-based binary vector [23] between its left and right T-DNA borders and a tandem 35S promoter and 35S terminator for subsequent agroinoculation and transcription of the viral infectious RNA; to enhance the infectivity of these transcripts, the 35S terminator was preceded by self-cleaving ribozyme sequence from the hepatitis delta virus [32] to remove the polyA sequence generated by the 35S terminator as polyA tracts can be detrimental to tobamoviruses [33] (Fig. 1B). pTVCV contained the wild-type TVCV cDNA and pTVCV-GFP contained the GFP transgene expression cassette—composed of the TMV CP subgenomic promoter, the GFP coding sequence, and the pseudoknot portion of the TMV 3′UTR for expression enhancement—inserted between the native TVCV MP subgenomic promoter and another, duplicated TVCV MP subgenomic promoter inserted upstream of MP and CP (Fig. 1B). Noteworthy, the first TVCV MP subgenomic promoter overlaps the coding sequence of the RNA-dependent RNA polymerase (RdRp) domain by ca. 150 nucleotides [34] and its presence is required for the RdRp activity whereas the second TVCV MP subgenomic promoter is necessary to drive transcription of MP and CP (Fig. 1B) and preserve the MP/CP gene overlap proposed to facilitate infection of crucifers [11], including Arabidopsis. The pTVCV-GFP variant is useful for visualizing the process of viral infection, from the initial local, cell-to-cell movement to subsequent systemic transport throughout the plant. In addition, pTVCV-GFP is important for testing the effects of the transgene "cargo" and the location of its placement within the viral sequence on the infectivity of the virus.

The infectivity of both pTVCV and pTVCV-GFP was tested in *N. benthamiana* plants. For assessing the spread of infection, lower

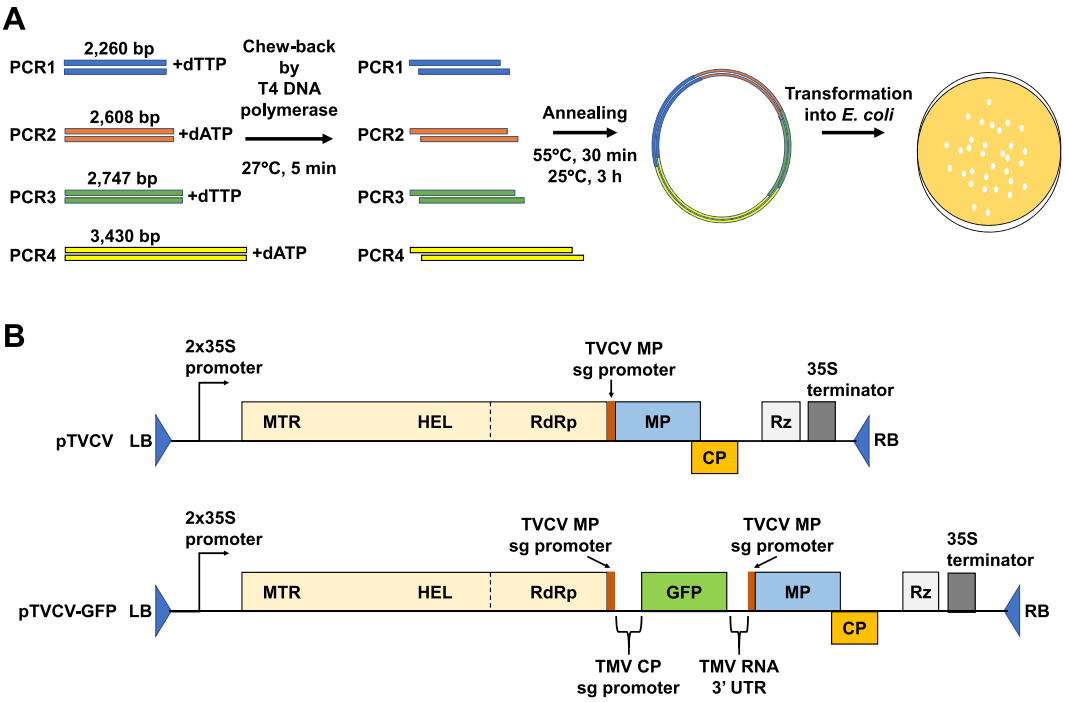

Fig. 1. Schematic illustration of the main steps of the restriction-ligation-independent cloning procedure and the resulting infectious TVCV clones. (A) Diagram of restriction-ligation-independent cloning of each of the PCR1-4 fragments to produce recessed DNA ends followed by fragment annealing for assembly into the pTVCV vector and transformation into *E. coli* cells. (B) Diagram of the structural and functional elements of the infectious pTVCV and the pTVCV-GFP vectors between the left (LB) and right T-DNA borders (RB) of the agroinoculation binary vector. MTR, methyltransferase domain; RNA helicase domain; RdRp, RNA-dependent RNA polymerase; MP, movement protein; CP, coat protein; Rz, ribozyme; sg, subgenomic.

leaves were agoinoculated with either pTVCV-GFP or with pTVCV that has no autofluorescent marker, and, for the negative control, the plants were mock-inoculated. Fig. 2A shows that neither mock-inoculated nor pTVCV-inoculated plants showed GFP fluorescence in any of their leaves and petioles whereas multiple systemic leaves and their petioles expressed clearly visible amounts of the fluorescent GFP signal in the pTVCV-GFP-inoculated plants. This GFP expression from the pTVCV-GFP infectious clone was confirmed on the cellular level by analyzing the expressing tissues by confocal microscopy. Fig. 2B shows that, in the systemic leaves of the pTVCV-GFP-inoculated plants, GFP accumulated in easily detectable amounts and in the typical nucleocytoplasmic pattern in all cells in the microscopic field of view, indicating efficient expression of the transgene. As expected, no GFP fluorescence was observed in cells from mock-inoculated plants or plants inoculated with pTVCV (Fig. 2B).

Examination of the infected *N. benthamiana* plants for the viral disease symptoms showed that both pTVCV and pTVCV-GFP infection produced characteristic wrinkling, stunting and mild chlorosis of the leaves (Fig. 2A). The typical symptoms of the TVCV infection [35,36] were also observed in Arabidopsis agroinoculated with either pTVCV or pTVCV-GFP. Fig. 3A shows that, compared to the mock-inoculated control plants, Arabidopsis inoculated with both variants of the TVCV infectious were markedly shorter with most systemic rosette leaves wrinkled and slightly chlorotic.

Finally, we examined the presence of the TVCV RNA in the pTVCV -and pTVCV-GFP-inoculated *N. benthamiana* plants. Our RT-PCR analysis of the systemic leaves did not detect viral RNA in the mock-inoculated plants but both pTVCV -and pTVCV-GFP-inoculated plants displayed easily detectable levels of the viral transcripts (Fig. 2C). The accumulation of the TVCV RNA was quantified using RT-qPCR. Fig. 2D shows that both constructs produced statistically significant levels of the viral RNA, with the pTVCV-GFP construct generating higher levels of the transcripts, making it an attractive platform for use as a gene expression vector.

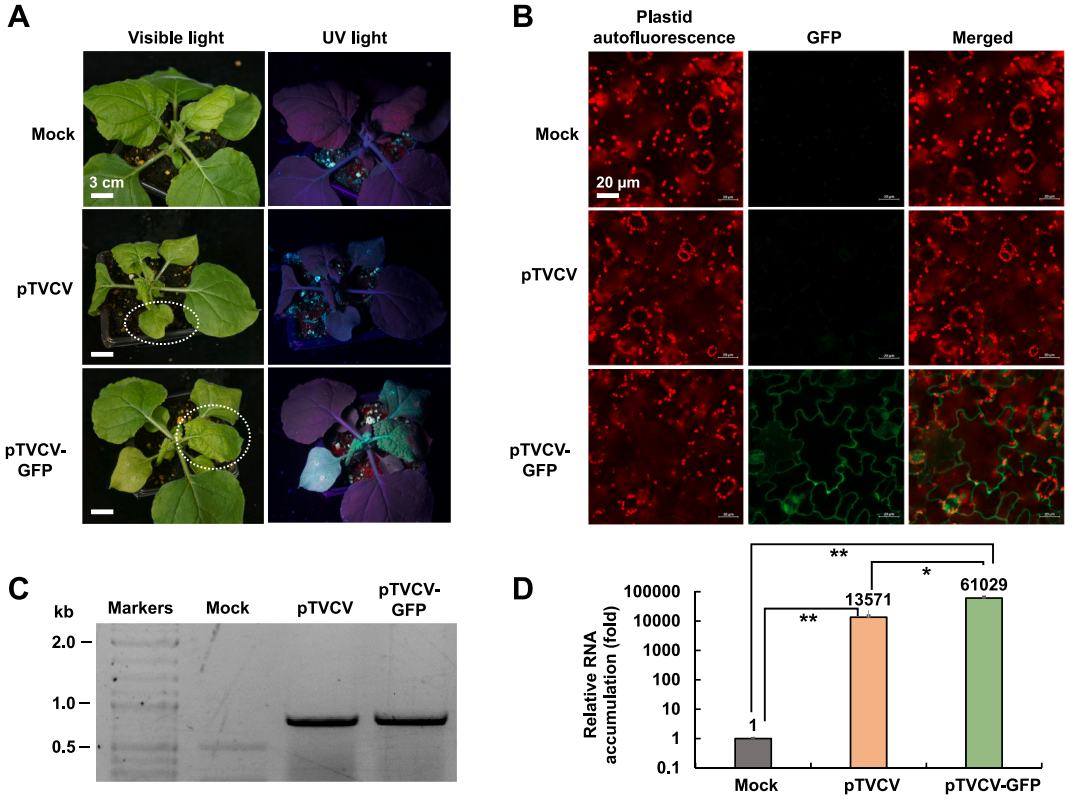

Fig. 2. Infectivity of the pTVCV and pTVCV-GFP clones in *N. benthamiana*. (A) Systemic symptom development and GFP expression in whole plants. Leaves were observed under visible light and representative symptomatic leaves are indicated by white dotted circles. GFP expression, visible as green fluorescence, was observed under UV light. Scale bars = 3 cm. (B) GFP expression in systemic leaf tissues. GFP signal is in green; chlorophyll autofluorescence is in red. All images are single confocal sections. Scale bars = 20 µm. (C) RT-PCR analysis of TVCV RNA accumulation in systemic leaves. The PCR products were resolved on a 1.0% agarose gel with molecular size markers indicated in kilobases (kb) on the left. The uncropped image of the agarose gel is shown in Fig. S1. (D) Relative accumulation of TVCV RNA quantified by RT-qPCR analysis of systemic leaves. The viral RNA level in mock-inoculated leaves was set as 1.0. Differences between mean values assessed by the two-tailed unpaired *t*-test are statistically significant for the p-values *$p < 0.05$ and **$p < 0.01$. The numerical values for individual data points used for this analysis are listed in Table S2. The RT-PCR and RT-qPCR were performed using the MP-specific primers detailed in Table S1. Plants were mock-inoculated (Mock) or agro-inoculated with pTVCV or pTVCV-GFP and analyzed at 4 dpi.

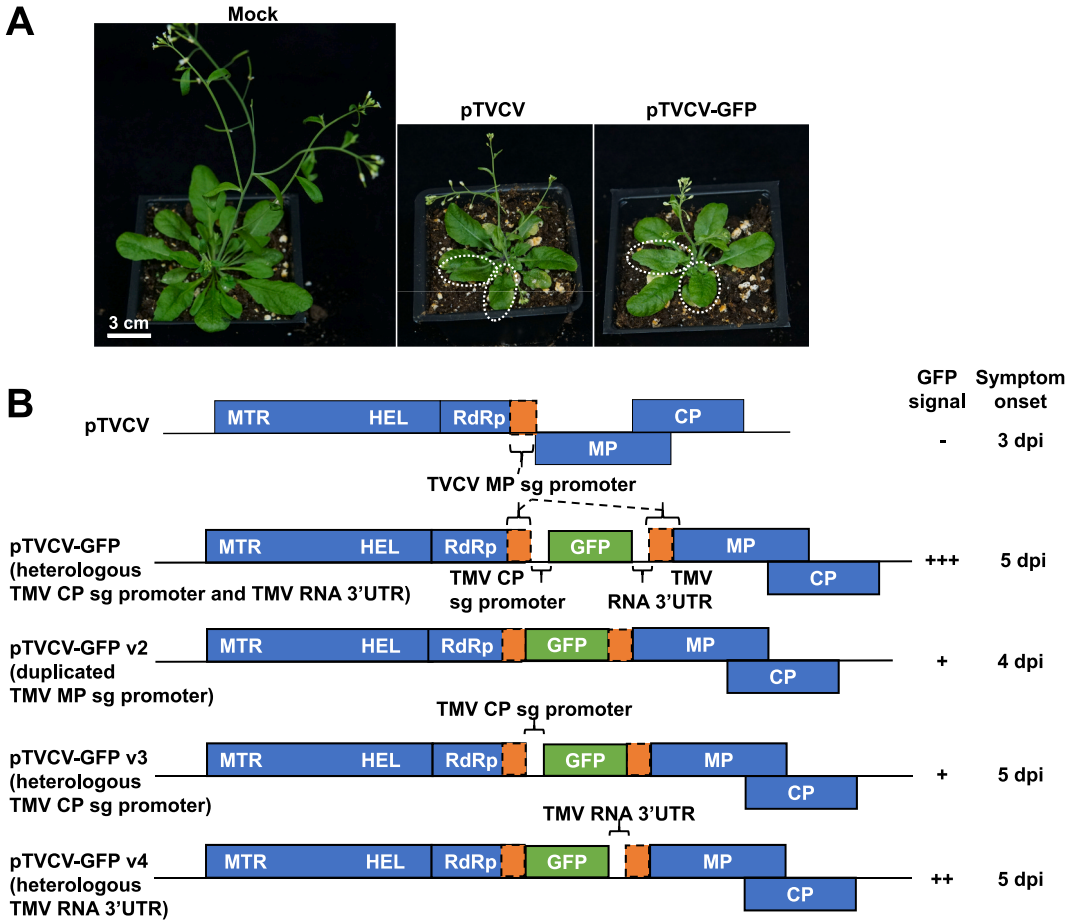

Fig. 3. Symptoms of the pTVCV and pTVCV-GFP infection in Arabidopsis and analyses of the roles of *cis*-acting regulatory sequences in the GFP transgene expression from the infectious pTVCV-GFP clone. (A) Symptoms of TVCV infection of Arabidopsis plants inoculated with pTVCV and pTVCV-GFP. Plants were mock-inoculated (Mock) or agroinoculated with pTVCV or pTVCV-GFP and analyzed at 14 dpi. Representative symptomatic systemic rosette leaves are indicated by white dotted circles. Scale bar = 3 cm. (B) Diagram of different combinations of TVCV and TMV subgenomic (sg) promoters and TMV 3UTR sequences in pTVCV-GFP and its v2–v4 variants. *N. benthamiana* plants were inoculated with the indicated infectious constructs and GFP expression in whole plants was detected as described in Fig. 2A. GFP detection was performed at the onset of infection symptoms which occurred at the indicated dpi times. Semiquantitative evaluation of GFP expression based on the visible intensity of GFP fluorescence: (−) no expression; (+++) strong expression; (+) weak expression; (++) intermediate expression. MTR, methyltransferase domain; RNA helicase domain; RdRp, RNA-dependent RNA polymerase; MP, movement protein; CP, coat protein.

3.2. *Configuration of the cis-acting regulatory sequences for transgene expression from the infectious TVCV clone*

pTVCV-GFP expresses the GFP transgene from an expression cassette that contains two heterologous regulatory sequences from another tobamovirus TMV, i.e., the CP subgenomic promoter and the pseudoknot of the 3′UTR (Fig. 3B). Before incorporating these regulatory elements into the expression vector, we examined their individual contributions to the efficiency of transgene expression. To this end, we generated three variants of the expression cassette in pTVCV-GFP: no CP subgenomic promoter and no pseudoknot 3′UTR (pTVCV-GFP v2), no pseudoknot 3′UTR (pTVCV-GFP v3), and no CP subgenomic promoter (pTVCV-GFP v4); in pTVCV-GFP v2 and pTVCV-GFP v4, the GFP expression is controlled by the native TVCV MP subgenomic promoter (Fig. 3B). We then compared the intensity of the GFP signal at the time of the symptom onset in *N. benthamiana* inoculated with pTVCV-GFP v2, pTVCV-GFP v4, and pTVCV-GFP v4 to those observed following inoculation with pTVCV-GFP and, as control, pTVCV. Fig. 3B shows that the presence of the TMV pseudoknot 3′UTR had the most effect on the pTVCV-GFP functionality, with the pTVCV-GFP v2 and pTVCV-GFP v3 producing the least intensity of the GFP signal, relative to pTVCV-GFP. The absence of the TMV CP subgenomic promoter in the presence of the TMV pseudoknot 3′UTR in pTVCV-GFP v4, on the other hand, yielded an intermediate GFP signal, suggesting that the heterologous promoter is less critical for the transgene expression yet is useful to augment the native TVCV MP subgenomic promoter in the pTVCV sequence. Thus, we adopted the composition and arrangement of the native and heterologous subgenomic promoters and 3′UTR of pTVCV-GFP for the construction of the TVCV-based expression vector.

3.3. Development of TVCV-based gateway-compatible infectious gene expression vector

Consistent with the restriction-ligation-independent assembly of the pTVCV-GFP infectious clone, its conversion to an expression vector was performed by introducing a Gateway cassette for recombination-based, restriction-ligation-independent cloning of genes of interest [24,37,38]. In the functional configuration of pTVCV-GFP, the Gateway cassette, designed to add a 3xFLAG epitope tag to the amino terminus of the expressed protein [24], was placed between the TMV CP subgenomic promoter and the TMV 3′UTR sequence (Fig. 4A, top schematic). This construct, designated pTVCV-DEST, represents the TVCV-based vector for transgene expression. Gateway-adapted ER-targeted mRFP reporter served as a model transgene which was recombined into pTVCV-DEST, resulting in the pTVCV-DEST-ER-mRFP vector (Fig. 4A, bottom schematic).

Our RT-PCR analysis of the TVCV transcripts showed that both pTVCV-DEST and pTVCV-DEST-ER-mRFP constructs functioned as infectious viral clones, accumulating statistically significant levels of the viral RNA in the systemic leaves (Fig. 4B); as expected no TVCV RNA was detected in mock-inoculated plants (Fig. 4B, top panel). Quantification of the viral RNA accumulation in the systemic leaves by RT-qPCR confirmed the infectivity of both constructs (Fig. 4B, bottom panel); interestingly and similar to the pTVCV -and pTVCV-GFP infectious clones, the "empty" vector pTVCV-DEST produced somewhat lower amounts of the viral RNA than the "loaded" pTVCV-DEST-ER-mRFP construct (compare Fig. 4B, bottom panel to Fig. 2D). Finally, we confirmed the functionality of pTVCV-DEST-

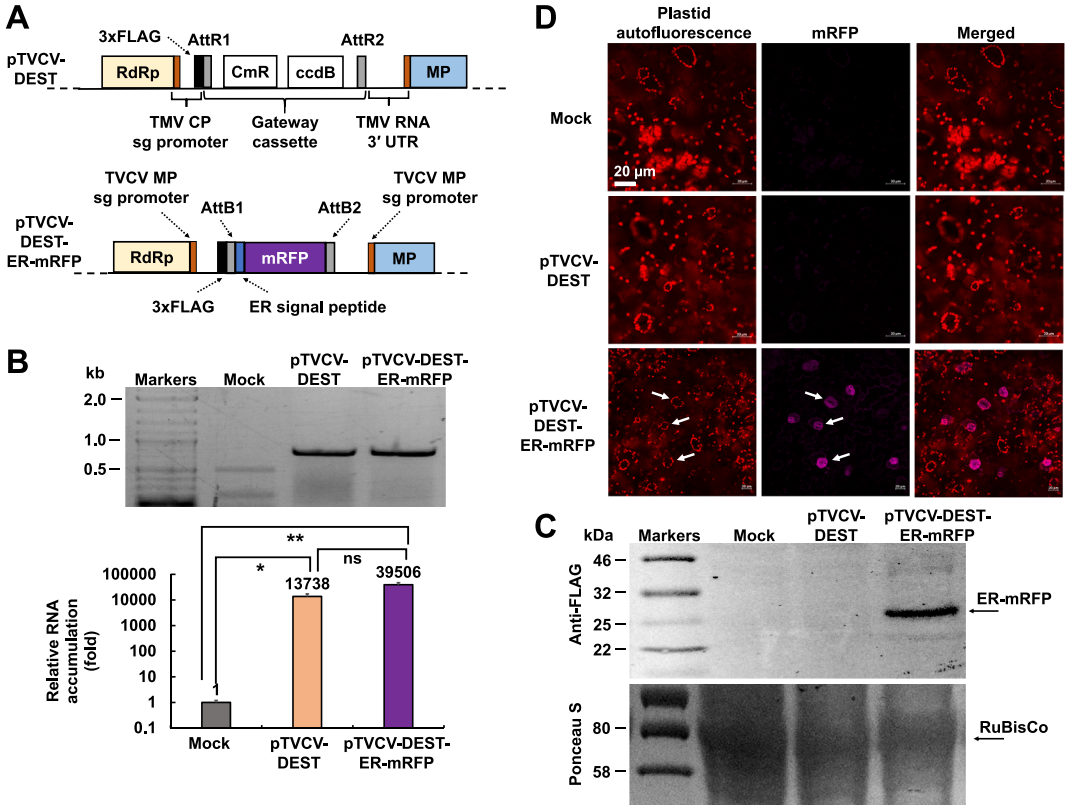

Fig. 4. Structure and functional characterization of TVCV-based Gateway-compatible infectious gene expression vector. (A) Schematic structure of pTVCV-DEST and pTVCV-DEST-ER-mRFP focusing on the location of the Gateway cassette [24] in the pTVCV infectious clone. RdRp, RNA-dependent RNA polymerase; MP, movement protein; CP, coat protein; sg, subgenomic. (B) Top panel. RT-PCR analysis of TVCV RNA accumulation in systemic leaves. The PCR products were resolved on a 1.0% agarose gel with molecular size markers indicated in kilobases (kb) on the left. The uncropped image of the agarose gel is shown in Fig. S1. Bottom panel. Relative accumulation of TVCV RNA quantified by RT-qPCR analysis of systemic leaves. The viral RNA level in mock-inoculated leaves was set as 1.0. Differences between mean values assessed by the two-tailed unpaired *t*-test are statistically significant for the p-values *$p < 0.05$ and **$p < 0.01$; $p \geq 0.05$ is not statistically significant (ns). The numerical values for individual data points used for this analysis are listed in Table S3. The RT-PCR and RT-qPCR were performed using the MP-specific primers detailed in Table S1. (C) Western blot analysis of the accumulation of ER-mRFP produced by pTVCV-DEST-ER-mRFP. Upper panel. Systemic leaves at 4 dpi were probed with anti-FLAG antibodies. Lower panel. Ponceau S staining of RuBisCo to assess relative loading of samples. Mock, mock-inoculated plants. The expected electrophoretic mobilities of ER-mRFP and RuBisCo (ribulose-1,5-bisphosphate carboxylase/oxygenase) are indicated by arrows on the right. Protein molecular mass markers are shown in kilodaltons on the left. The uncropped images of the blots are shown in Fig. S1. (D) ER-mRFP expression in systemic leaf tissues of plants inoculated with pTVCV-DEST or pTVCV-DEST-ER-mRFP. mRFP signal is in magenta; chlorophyll autofluorescence is in red. Arrows indicate some of the stomata that express ER-mRFP. All images are single confocal sections. Scale bars = 20 µm. Plants were mock-inoculated (Mock) or agroinoculated with pTVCV-DEST or pTVCV-DEST-ER-mRFP and analyzed at 4 dpi.

ER-mRFP by Western blotting using anti-FLAG antibodies. These experiments revealed accumulation of the FLAG-tagged ER-mRFP protein in the systemic leaves of plants inoculated with pTVCV-DEST-ER-mRFP, but not in mock-inoculated plants or in plants inoculated with pTVCV-DEST (Fig. 4C).

Ultimately, the pTVCV-DEST-ER-mRFP construct would be useful mainly to express and visualize the autofluorescent marker in plant tissues. Fig. 4D shows that our confocal microscopy analysis of systemic leaves of *N. benthamiana* inoculated with pTVCV-DEST-ER-mRFP detected numerous cells expressing and accumulating ER-mRFP; interestingly, unlike the free GFP reporter (Fig. 2B), the main accumulation of the ER-targeted mRFP reporter occurred in stomatal cells (Fig. 4D, arrows), consistent with the observation that TVCV infection affects the host plant stomata [39]. No ER-mRFP signal was observed in negative controls, i.e., following mock-inoculation or inoculation with pTVCV-DEST (Fig. 4D).

Collectively, our data indicate that our restriction-ligation-independent protocols are useful to produce an infectious TVCV clone directly from the viral genomes purified from infected tissues and suggest that a similar approach can be applied to other plant viruses isolated in the field. Subsequently, the TVCV infectious clone was deployed as a platform for the generation of an infectious TVCV-based gene expression vector that systemically infects plants and expresses a transgene of interest. The systemic spread of the pTVCV, pTVCV-DEST, and pTVCV-DEST-ER-mRFP vectors (Figs. 2–4) suggests that the virions moving through and replicating in numerous cells retain their functionality and, by implication, the stability of their genomes. Our data also delineate the functional configuration of the *cis*-acting elements that regulate the transgene expression from the TCVC-based vector. Generally, the adaptation of viral genomes for the expression of foreign proteins involves either the introduction of a heterologous promoter from a related virus or the duplication of the native subgenomic promoter to drive the expression of the transgene [40]. Here, we combined both approaches, i.e., in pTVCV-DEST, the transgene expression is controlled by the tandem of the native TVCV MP subgenomic promoter and the downstream heterologous TMV CP promoter as well as by the heterologous TMV 3′UTR pseudoknot placed upstream of the duplicated TVCV MP subgenomic promoter, further preserving the sequence overlap between the native MP and CP genes overlap suggested to favor the viral infectivity [11]. Broadly, this work also would be useful for the construction of expression vectors based on a model tobamovirus that readily infects *N. benthamiana* and Arabidopsis model hosts and for the deployment of the restriction-ligation-independent cloning to assemble infectious clones of RNA viruses.

3.4. Limitations of study

This study represents the initial report of a restriction-ligation-independent approach to generate an infectious clone of TVCV and a TVCV-based gene expression vector for plants. Therefore, necessarily, it does not include detailed and extensive characterization of the generated expression vector, such as kinetics of transgene expression, transgene expression in different tissues and cell types, and expression of different transgenes. In addition, the described approach has not been tested for other, unrelated RNA viruses.

Ethics statement

Review and/or approval by an ethics committee was not needed for this study because it did not include human or animal subjects. Informed consent was not required for this study because it did not include human subjects.

Author contribution statement

Andrea Mirauti: Conceived and designed the experiments; Performed the experiments; Analyzed and interpreted the data; Wrote the paper.

Phu-Tri Tran: Conceived and designed the experiments; Performed the experiments; Analyzed and interpreted the data; Contributed reagents, materials, analysis tools or data; Wrote the paper.

Vitaly Citovsky: Conceived and designed the experiments; Analyzed and interpreted the data; Wrote the paper.

Data availability statement

Data included in article/supp. material/referenced in article.

Declaration of competing interest

The authors declare that they have no known competing financial interests or personal relationships that could have appeared to influence the work reported in this paper.

Acknowledgments

The work in the V.C. laboratory was supported by grants from NIH (R35 GM144059, R01 GM50224), NSF (MCB 1913165), NSF/NIFA (IOS 1758046), and BARD, Israel (IS-5276-20) to V.C.

Appendix A. Supplementary data

Supplementary data to this article can be found online at https://doi.org/10.1016/j.heliyon.2023.e19855.

References

[1] K. Hefferon, Plant virus expression vector development: new perspectives, BioMed Res. Int. (2014), 785382, https://doi.org/10.1155/2014/785382, 2014.
[2] K. Hefferon, Plant virus expression vectors: a powerhouse for global health, Biomedicines 5 (2017) 44, https://doi.org/10.3390/biomedicines5030044.
[3] S.S. Zaidi, S. Mansoor, Viral vectors for plant genome engineering, Front. Plant Sci. 8 (2017) 539, https://doi.org/10.3389/fpls.2017.00539.
[4] P. Abrahamian, et al., Plant virus-derived vectors: applications in agricultural and medical biotechnology, Annu. Rev. Virol. 7 (2020) 513–535, https://doi.org/10.1146/annurev-virology-010720-054958.
[5] N. Brisson, et al., Expression of a bacterial gene in plants by using a viral vector, Nature 310 (1984) 511–514.
[6] R. Lartey, et al., Movement and subcellular localization of a tobamovirus in *Arabidopsis*, Plant J. 12 (1997) 537–545.
[7] R.T. Lartey, et al., Occurrence of a vein-clearing tobamovirus in turnip, Plant Dis. 77 (1993) 21–24.
[8] R.T. Lartey, et al., Completion of a cDNA sequence from a tobamovirus pathogenic to crucifers, Gene 166 (1995) 331–332.
[9] I. Aguilar, et al., Nucleotide sequence of *Chinese rape mosaic virus* (oilseed rape mosaic virus), a crucifer tobamovirus infectious on *Arabidopsis thaliana*, Plant Mol. Biol. 30 (1996) 191–197.
[10] R. Lartey, et al., Tobamovirus evolution: gene overlaps, recombination and taxonomic implications, Mol. Biol. Evol. 13 (1996) 1327–1338.
[11] Y.L. Dorokhov, et al., Tobamovirus 3'-terminal gene overlap may be a mechanism for within-host fitness improvement, Front. Microbiol. 8 (2017) 851, https://doi.org/10.3389/fmicb.2017.00851.
[12] R.R. Chavan, M.N. Pearson, Molecular characterisation of a novel recombinant *Ribgrass mosaic virus* strain FSHS, Virol. J. 13 (2016) 29, https://doi.org/10.1186/s12985-016-0487-5.
[13] J.L. Schmid-Burgk, et al., A ligation-independent cloning technique for high-throughput assembly of transcription activator-like effector genes, Nat. Biotechnol. 31 (2013) 76–81.
[14] J. Stevenson, et al., A practical comparison of ligation-independent cloning techniques, PLoS One 8 (2013), e83888, https://doi.org/10.1371/journal.pone.0083888.
[15] Y. Wang, et al., Restriction-ligation-free (RLF) cloning: a high-throughput cloning method by *in vivo* homologous recombination of PCR products, Genet. Mol. Res. 14 (2015) 12306–12315, https://doi.org/10.4238/2015.October.9.19.
[16] J. Yang, et al., A ligation-independent cloning method using nicking DNA endonuclease, Biotechniques 49 (2010) 817–821, https://doi.org/10.2144/000113520.
[17] J.Y. Jeong, et al., One-step sequence- and ligation-independent cloning as a rapid and versatile cloning method for functional genomics studies, Appl. Environ. Microbiol. 78 (2012) 5440–5443, https://doi.org/10.1128/AEM.00844-12.
[18] J.L. Schmid-Burgk, et al., Rapid hierarchical assembly of medium-size DNA cassettes, Nucleic Acids Res. 40 (2012) e92, https://doi.org/10.1093/nar/gks236.
[19] S. Ueki, et al., Functional transient genetic transformation of *Arabidopsis* leaves by biolistic bombardment, Nat. Protoc. 4 (2009) 71–77.
[20] I. Keren, et al., Histone deubiquitinase OTU1 epigenetically regulates *DA1* and *DA2*, which control *Arabidopsis* seed and organ size, iScience 23 (2020), 100948.
[21] P.T. Tran, V. Citovsky, Receptor-like kinase BAM1 facilitates early movement of the *Tobacco mosaic virus*, Commun. Biol. 4 (2021) 511, https://doi.org/10.1038/s42003-021-02041-0.
[22] Y. Zhang, et al., Limitations to tobacco mosaic virus infection of turnip, Arch. Virol. 144 (1999) 957–971.
[23] J.A. Lindbo, TRBO: a high-efficiency *Tobacco mosaic virus* RNA-based overexpression vector, Plant Physiol. 145 (2007) 1232–1240, https://doi.org/10.1104/pp.107.106377.
[24] S. Kagale, et al., TMV-Gate vectors: gateway compatible tobacco mosaic virus based expression vectors for functional analysis of proteins, Sci. Rep. 2 (2012) 874, https://doi.org/10.1038/srep00874.
[25] E.M. Bahassi, et al., Interactions of CcdB with DNA gyrase. Inactivation of GyrA, poisoning of the gyrase-DNA complex, and the antidote action of CcdA, J. Biol. Chem. 274 (1999) 10936–10944.
[26] B. Lacroix, V. Citovsky, Extracellular VirB5 enhances T-DNA transfer from *Agrobacterium* to the host plant, PLoS One 6 (2011), e25578.
[27] T. Kowalczyk, et al., High efficiency transformation of *Brassica oleracea* var. *botrytis* plants by *Rhizobium rhizogenes*, Amb. Express 8 (2018) 125, https://doi.org/10.1186/s13568-018-0656-6.
[28] P.T. Tran, et al., A plant intron enhances the performance of an infectious clone *in planta*, J. Virol. Methods 265 (2019) 26–34.
[29] M.W. Lee, Y. Yang, Transient expression assay by agroinfiltration of leaves, Methods Mol. Biol. 323 (2006) 225–229.
[30] P.T. Tran, et al., Isolation and validation of a candidate *Rsv3* gene from a soybean genotype that confers strain-specific resistance to soybean mosaic virus, Virology 513 (2018) 153–159.
[31] K.J. Livak, T.D. Schmittgen, Analysis of relative gene expression data using real-time quantitative PCR and the 2(-delta delta C(T)) method, Methods 25 (2001) 402–408.
[32] C.H. Webb, A. Luptak, HDV-like self-cleaving ribozymes, RNA Biol. 8 (2011) 719–727, https://doi.org/10.4161/rna.8.5.16226.
[33] S. Guo, et al., TMV mutants with poly (A) tracts of different lengths demonstrate structural variations in 3′ UTR affecting viral RNAs accumulation and symptom expression, Sci. Rep. 5 (2015) 1–12.
[34] E. Knapp, D.J. Lewandowski, *Tobacco mosaic virus*, not just a single component virus anymore, Mol. Plant Pathol. 2 (2001) 117–123.
[35] A. Uchiyama, et al., The *Arabidopsis* synaptotagmin SYTA regulates the cell-to-cell movement of diverse plant viruses, Front. Plant Sci. 5 (2014) 584.
[36] P. Gyula, et al., Ecotype-specific blockage of tasiARF production by two different RNA viruses in *Arabidopsis*, PLoS One 17 (2022), e0275588, https://doi.org/10.1371/journal.pone.0275588.
[37] M. Karimi, et al., GATEWAY vectors for *Agrobacterium*-mediated plant transformation, Trends Plant Sci. 7 (2002) 193–195.
[38] A.J. Walhout, et al., GATEWAY recombinational cloning: application to the cloning of large numbers of open reading frames or ORFeomes, Methods Enzymol. 328 (2000) 575–592.
[39] R.R. Murray, et al., Plant virus infections control stomatal development, Sci. Rep. 6 (2016), 34507, https://doi.org/10.1038/srep34507.
[40] P.T. Tran, et al., Rapid generation of inoculum of a plant RNA virus using overlap PCR, Virology 553 (2021) 46–50, https://doi.org/10.1016/j.virol.2020.11.001.